

Estimating the snow distribution in a subalpine region using a distributed snowmelt model

KENTARO MATSUI

Graduate School of Agriculture, Iwate University, Uyeda 3-18, Morioka, Iwate 020-8550, Japan and Graduate School of Bioggricultural Sciences, Nagoya University, Furo-cho, Chikusa-ku, Nagoya, Aichi 464-8601, Japan

TAKESHI OHTA

Graduate School of Bioggricultural Sciences, Nagoya University, Furo-cho, Chikusa-ku, Nagoya, Aichi 464-8601, Japan
takeshi@agr.nagoya-u.ac.jp

Abstract A distributed snowmelt model was applied to a subalpine region. The model is based on an energy budget method and evaluates topography and vegetation cover. In the Akagawa basin, Japan, the model reproduced the proportion of snow coverage and snow water equivalent in the snowmelt season exactly. The simulated results agreed better at forest sites than at open sites, and at lower sites rather than at higher sites. This suggests that the snow redistribution caused by wind cannot be ignored in predicting snow distribution in a subalpine zone.

Key words distributed snowmelt model; heat balance; spatial snow distribution; subalpine; temporal snow distribution

INTRODUCTION

Estimating the snow distribution in subalpine regions is important for managing water resources. Recently, many methods using remote sensing technology, such as the interpretation of aerial photographs or satellite images, have been proposed for observing snow distribution. These methods are effective in places where the vegetation density is low. However, when such techniques are used for dense forest, it is difficult to determine the snow distribution on the ground below the forest canopy and to determine the temporal change in snow properties. In order to avoid these problems, we used a heat-balance method to simulate snow accumulation and melt. By considering the balance in snow accumulation between precipitation and snowmelt runoff using a heat balance method, we were able to estimate the snow water equivalent and judge the snow coverage at arbitrary points.

This paper discusses the snow distribution in a subalpine region using a distributed snowmelt model that considers vegetation density; this study also verifies the performance of the model for two winters by comparing the difference in snow water equivalents at open and forest sites.

STUDY AREA

Our study area was the Akagawa basin, located in Hachimantai Semi-National Park, in northwest Iwate Prefecture, Japan, at 39°57'N, 140°55'E (Fig. 1). The basin covers

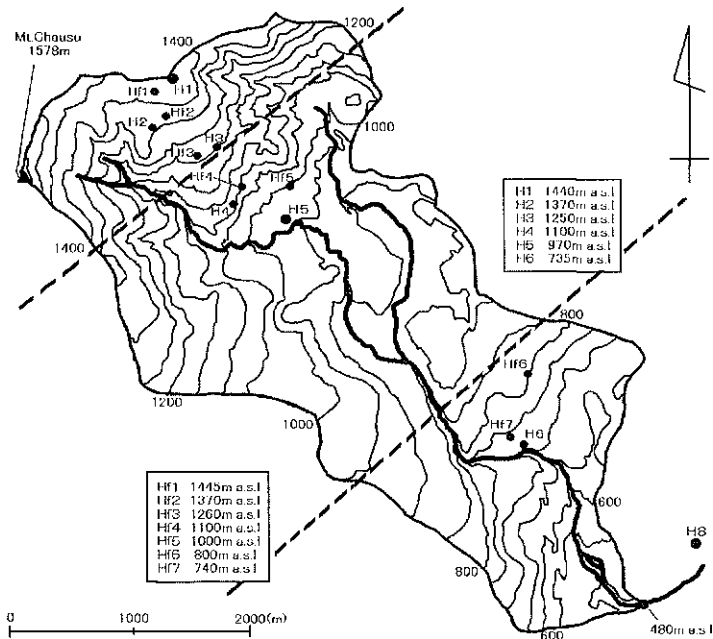


Fig. 1 Contour map of the Akagawa basin; contour interval: 50 m. The broken lines in this figure are the boundaries of each of the domains for which X in equation (5) is calculated.

16.7 km² and the elevation ranges from 480 to 1578 m a.s.l. Evergreen conifers cover the part of the basin above 1100 m a.s.l., and deciduous trees cover lower areas. These forests are generally sparse and the areas without forest are dominated by bamboo grass. The average height of trees throughout the basin is about 8 m.

In this basin, the maximum snow water equivalent exceeds 1000 mm annually, but most of the snow coverage disappears by the end of May due to the intense snowmelt that begins in the middle of April.

There are three meteorological observation stations in or near the basin: H1, H5, and H8 (Fig. 1). Air temperature, relative humidity, insolation and wind speed were measured at these stations. In addition, precipitation was measured at H5. These five parameters were used to determine the snowmelt rate and snow water equivalent in the basin. Furthermore, during the winters of 1998–1999 and 1999–2000, we conducted intensive observations to measure the snow water equivalent at a total of 13 sites. In Fig. 1, sites H1 to H6 are open sites, and sites Hf1 to Hf7 are forest sites. In addition, hemispherical photographs were taken at these sites in the same period using a fish-eye lens to determine the vegetation coverage ratio.

METHOD

This study used the distributed snowmelt model devised by Ohta (1994), which considers the snowpack as a single bulk layer, and estimates the snowmelt rate as influenced by differences in forest conditions. Dividing a basin into a grid of arbitrary

size, the model calculates the snowmelt energy at a certain point as a representative value for the corresponding grid. For the analysis, we used a 100-m grid based on the 50-m DEM grid published by the Geographical Survey Institute.

Description of forest conditions in the model

The heat balance at the snow surface is controlled by meteorological elements which vary with forest conditions. Therefore, the heat balance in each grid is calculated after considering the changes in the meteorological elements resulting from differences in the forest conditions. In this analysis, we express the difference in forest conditions as the difference in a sky factor. In order to determine the sky factor at arbitrary points, we used an orthographic aerial photograph taken when the entire basin was snow covered. As this photograph was taken during fine weather, the white areas indicate snow coverage and the black portions are forest. Therefore, in each grid, the ratio of white to black is an index expressing the forest density in each grid. By comparing the proportion of white in some of the 100-m grids obtained from the orthographic aerial photograph, and the sky factor at the same points obtained from hemispherical photographs taken using a fish-eye lens, the sky factor at the arbitrary point in the basin is expressed as:

$$\beta = 0.83\alpha + 0.17 \quad (1)$$

where α is the proportion of white in a given 100-m grid and β is the sky factor at a zenith angle of 84° for the same grid. Assuming that the average height of a tree in the 100-m grid is 8 m, a zenith angle of 84° reflects only the trees inside a grid.

Description of the meteorological elements in the model

The meteorological elements related to snowmelt are influenced by the terrain, and change with differences in location. In this study, the predicted values of three elements, temperature, humidity and wind speed, are described as a function of altitude using:

$$X_e(h) = X_{H5} + f \cdot \frac{h-970}{100} \quad (2)$$

where X_e is the estimated value of each meteorological element at h m a.s.l.; X_{H5} is the meteorological value measured at H5; and f is the rate of change in each meteorological element with a vertical drop of 100 m, and is expressed by the following equation:

$$f = (X_{H1} - X_{H5}) / \frac{(1440 - 970)}{100} \quad (3)$$

$$f = (X_{H5} - X_{H8}) / \frac{(970 - 450)}{100} \quad (4)$$

where X_{H1} and X_{H8} are the meteorological measurements at H1 and H8, respectively. By calculating the value of f at every measurement time, the rate of change with altitude, at that moment, can be expressed.

Local clouds influence insolation. In this analysis the cover effect of insolation by local clouds was expressed by considering the ratio of the daily insolation on a fine day at the observation site, and the daily insolation measured at each point. The relationship between the daily insolation measured at each observation point, $\sum I$, and the daily insolation for a fine day, $\sum I_{Fine}$, is as follows:

$$\sum I = X \cdot \sum I_{Fine} \tag{5}$$

where, X is a coefficient expressing the attenuation of insolation, and takes a value from 0.0 to 1.0. It was assumed that the insolation observed at H1, H5, and H8 was representative of the three domains shown in Fig. 1, which each include an observation site. X is calculated from the domain each day, and remains constant for the day. Therefore, the hourly insolation, I , of one grid belonging to each domain is as follows:

$$I = I_{dr} + I_{df} \tag{6}$$

$$I_{dr} = I_o P^{\frac{1}{\sin h_s}} (\sin h_s \cos \theta + \cos h_s \sin \theta \cos(D - b)) \tag{7}$$

$$I_{df} = \frac{1}{2} I_o \sin h_s \left(\frac{1 - P^{\frac{1}{\sin h_s}}}{1 - 1.4 \ln P} \right) \frac{(1 + \cos \theta)}{2} \tag{8}$$

where I_{dr} and I_{df} are the direct and diffuse radiation, respectively, I_o is the solar constant, P is the atmospheric transmittance ($= 0.77$, constant in the analysis), h_s is the sun angle, θ is the oblique angle of the hillslope, D is the angle of the direction of the sun, and b is the angle of the direction of the hill slope. For D and b , 0 is due south, and values to the west are positive. In addition, h_s and D are expressed using the following equations:

$$\sin h_s = \sin C_x \sin S + \cos C_x \cos S \cos t_x \tag{9}$$

$$\sin D = \frac{\cos S \sin t_x}{\cos h_s} \tag{10}$$

where C_x is the latitude in degrees, S is the solar declination, and t_x is the hour angle.

The precipitation $P(h)$ at h m a.s.l. is expressed as a function of altitude as follows:

$$P(h) = (1 + f_p (h - h_o)) \cdot P(h_o) \tag{11}$$

where, f_p is the rate of change in precipitation with altitude, and h_o is the altitude of the point at which precipitation is measured. Using the observed form of precipitation and terrestrial temperature, f_p is given by the following equations (Ohta, 1989):

$$f_p = 0 \quad (T_a \geq 1.75) \tag{12}$$

$$f_p = 0.001 \quad (T_a < 1.75) \tag{13}$$

where T_a is the air temperature in the grid derived from equation (2). The form of precipitation is judged to be rain when $T_a \geq 1.75$ and snow when $T_a < 1.75$; the value of f_p is given according to each form of precipitation.

Relationship between forest conditions and meteorological elements

In each grid, the meteorological values are presumed after considering the differences in the terrain, according to the influence of forest condition. In the analysis, we assumed that air temperature and humidity were not influenced significantly by forest. We considered the influence of forest conditions on three meteorological elements: insolation, wind speed, and downward longwave radiation.

In considering the effect of forest cover on insolation, the insolation in the forest, I_f , is given by:

$$I_f = I \beta \quad (14)$$

where I is the insolation obtained from equation (6), and β is the sky factor obtained using equation (1).

The wind speed in the forest, U_f , is derived by multiplying the wind speed, U , calculated using equation (2), by the coefficient B , which expresses the reduction in the wind speed with the existence of forest as follows:

$$U_f = U B \quad (15)$$

$$B = \exp(-1.39 PAI) \quad (16)$$

where, PAI is the plant area index. The PAI in a given grid can be found using the following equation (Suzuki *et al.*, 1999):

$$PAI = \ln(\beta_{90})/(-0.75) \quad (17)$$

where β_{90} is the sky factor at a zenith angle of 90° . From the hemispherical photographs taken in this basin, it is expressed by the following equation:

$$\beta_{90} = \beta^{1.35} \quad (18)$$

where β is the zenith angle derived using equation (1).

As the downward longwave radiation in the forest consists of the atmospheric longwave radiation and longwave radiation emitted by trees, the downward longwave radiation in the forest, L_f , is determined as follows (Ohta, 1993):

$$L_f = f_i L + (1 - f_i) \sigma (T_f + 273.15)^4 \quad (19)$$

where f_i is the transmittance of the canopy for atmospheric longwave radiation, L is the atmospheric longwave radiation, σ is the Stefan-Boltzmann constant, and T_f is the surface temperature of the trees. In this study, we assumed that f_i and T_f were equals, to equals to β and T_a , respectively. The atmospheric longwave radiation, L , is given by (Ohta, 1992):

$$L = (1 + 0.2(1 - Cc))(0.51 + 0.066e^{0.5}) \sigma (T_a + 273.15)^4 \quad (20)$$

$$Cc = 0.74 \frac{I_{obs}}{I_{top}} \quad (21)$$

where Cc is a factor representing clear sky, I_{obs} is the daily solar radiation measured at the observation sites, I_{top} is the daily solar radiation at the outer limit of the atmosphere, and T_a is the air temperature.

Calculating the heat balance for the entire snowpack

To calculate the heat balance for the entire snowpack, we used the heat balance model proposed by Kondo & Yamazaki (1990). In the snowmelt season, the snowmelt water near the snow surface refreezes with nocturnal cooling. Moreover, the freezing depth increases with cooling. Due to refreezing, when the heat balance becomes positive again, the snowmelt does not necessarily start immediately. This model can express the delay in the start of snowmelt with nocturnal cooling by considering freezing depth, Z , and surface temperature, T_s . In this model, the equation for the conservation of energy for the entire snowpack is written as:

$$\frac{1}{2} c_s \rho_s [Z(T_0 - T_s) - Z_n(T_0 - T_{sn})] + W_0 \rho_s l_f (Z - Z_n) + M_0 \Delta t = G \Delta t \quad (22)$$

where, c_s is the specific heat of ice, ρ_s is the snow density, W_0 is the maximum water content of the snowpack, l_f is the heat fusion of ice, M_0 is the energy required to create runoff from the snowpack, and Δt is the time step. After Δt passes, T_s and Z change to T_{sn} and Z_n , respectively. Here, the value of Δt is 1 h, and W_0 is 0.15. Moreover, ρ_s is computed using Kojima's theory (1957). G is the energy received by the entire snow pack through the snow surface and bottom, and is given by:

$$G = (1 - \alpha)I + L - \epsilon T_s^4 - H - lE + Q_r \quad (23)$$

where α is the albedo of the snow surface, ϵ is the snow emissivity, H , lE , and Q_r are the sensible heat, latent heat, and heat in rainfall, respectively. Here, ϵ is assumed constant (= 1.0) and Q_r is given by:

$$Q_r = 4.186 P T_a \quad (24)$$

where P is the hourly rainfall derived from equation (11), and T_a is the air temperature derived from equation (2). The sensible and latent heats are given by the following bulk formulas:

$$H = c_p \rho C_H U (T_s - T_a) \quad (25)$$

$$lE = l \rho C_E U [q_s(T_s) - q] \quad (26)$$

where c_p is the specific heat of air at a constant pressure, ρ is the air density, U is the wind speed, q is the specific humidity, and $q_s(T_s)$ is the saturated specific humidity at temperature T_s . C_H and C_E are the bulk coefficients for the sensible and latent heat, respectively. The values of C_H and C_E are expressed as a function of PAI following Suzuki *et al.* (1999):

$$C_H = C_E = 0.00147 PAI + 0.0023 \quad (27)$$

PAI can be derived from equation (17).

RESULTS AND DISCUSSION

Snow water equivalent in the open and forest sites

For the simulation that started on 5 January 2000, the initial conditions were given as a function of altitude, as shown in Fig. 2. At this time, snow already covered the entire

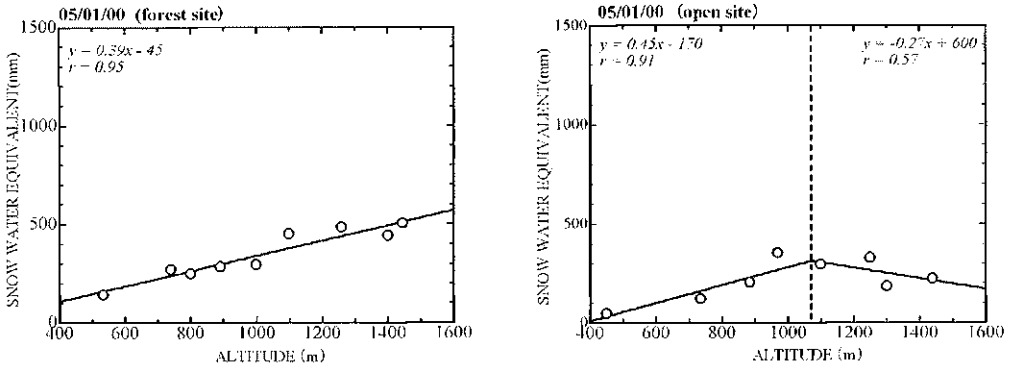


Fig. 2 The snow water equivalent on 5 January 2000; this snow water equivalent distribution was used as the initial condition for the simulation.

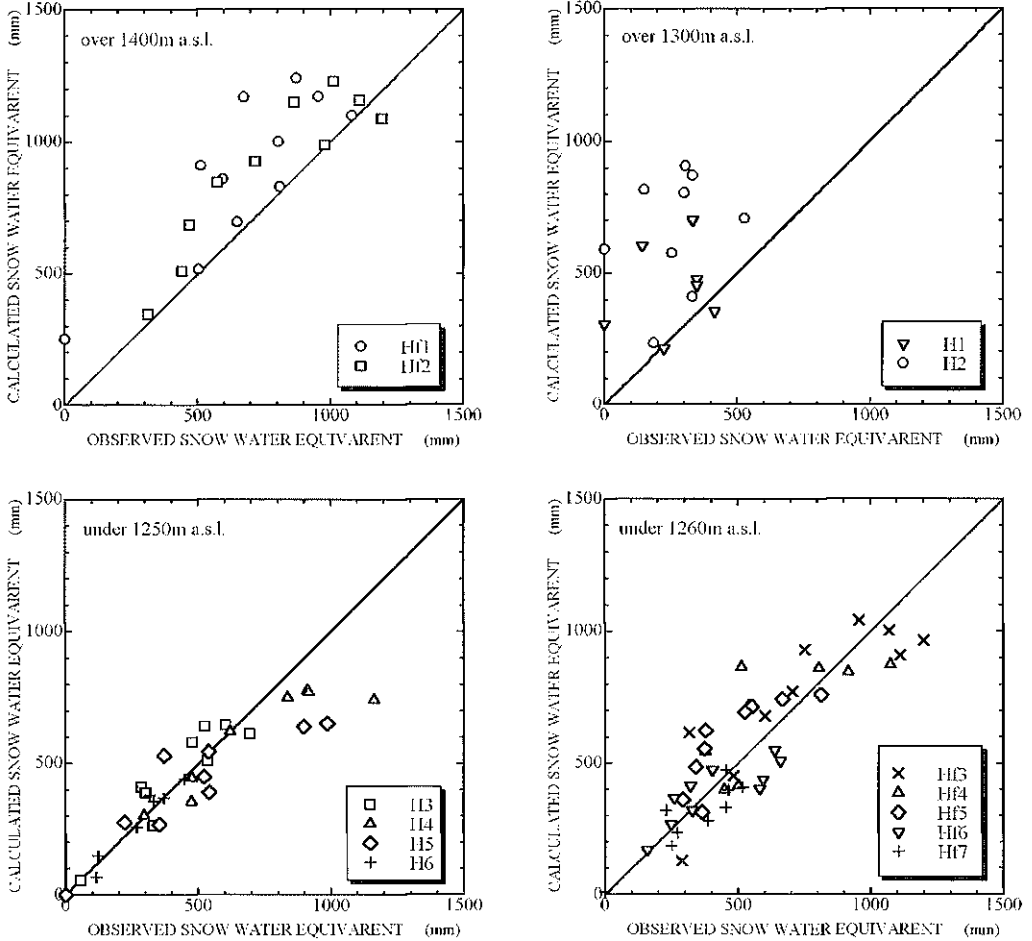


Fig. 3 Comparison of the calculated and observed results.

basin. Therefore, the results of the snow survey performed on the same day were used. Based on the observed results, different conditions for the open and forest sites were used. The calculated and observed results are compared in Fig. 3. There is good agreement at both the forest and open sites, except at the high altitude open sites. The agreement is better for the forest sites than for the open sites. Moreover, the calculated values are overestimates for the open sites at high altitude. One cause of this is thought to be the greater wind speed at open and higher sites vs forest and lower sites. Since snow is carried away by stronger winds, the snow water equivalent may decrease at such sites. Since this model does not consider snow redistribution, it is thought that it is less accurate for higher altitudes.

Spatial snow distribution

The spatial snow distribution was simulated using the conditions starting on 14 March 1999. The initial H_w in this analysis is shown in Fig. 4, and is described as a function of altitude, h , using:

$$H_w = (0.0047h - 2.6) \times (-0.0002h + 0.53) \times 1000 \tag{28}$$

Equation (28) is determined from the snow depth and the mean density of the entire layer measured at the same time. Since both the mean density of the entire layer and the snow depth were approximated by linear functions of altitude, the rate of increase in snow water equivalent decreases with increasing altitude (Fig. 4). Figure 5 shows the simulated and actual snow distribution on 1 May (47 days after the start of analysis) and 12 May 1999 (58 days after the start). The actual distribution was scanned from aerial photographs taken on the same days. Based on this figure, the basin was divided into zones at 100-m altitude intervals, and the relative snow cover in each zone was calculated. Figure 6 compares the actual and simulated rate of snow coverage for each altitude zone. On both 1 and 12 May, the altitude zones with snow coverage rates from 0.0 to 0.2 agreed very well. However, simulated values exceed the observed values for altitude zones with snow coverage of 0.4 or more. The difference was most marked for values from 0.3 to 0.6. This is thought to occur because the initial conditions were spatially homogeneous, irrespective of inequalities in the ground or forest conditions.

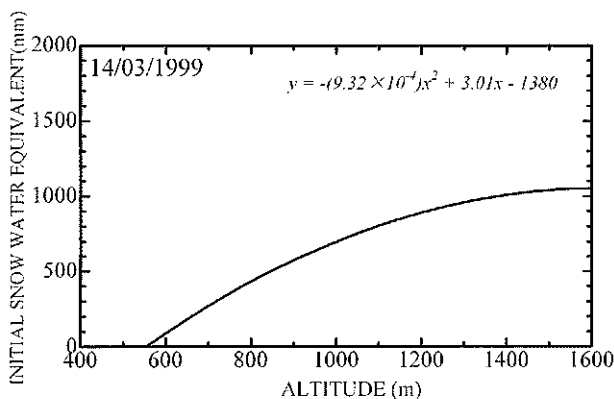


Fig. 4 Initial conditions for the simulation that started on 14 March 1999.

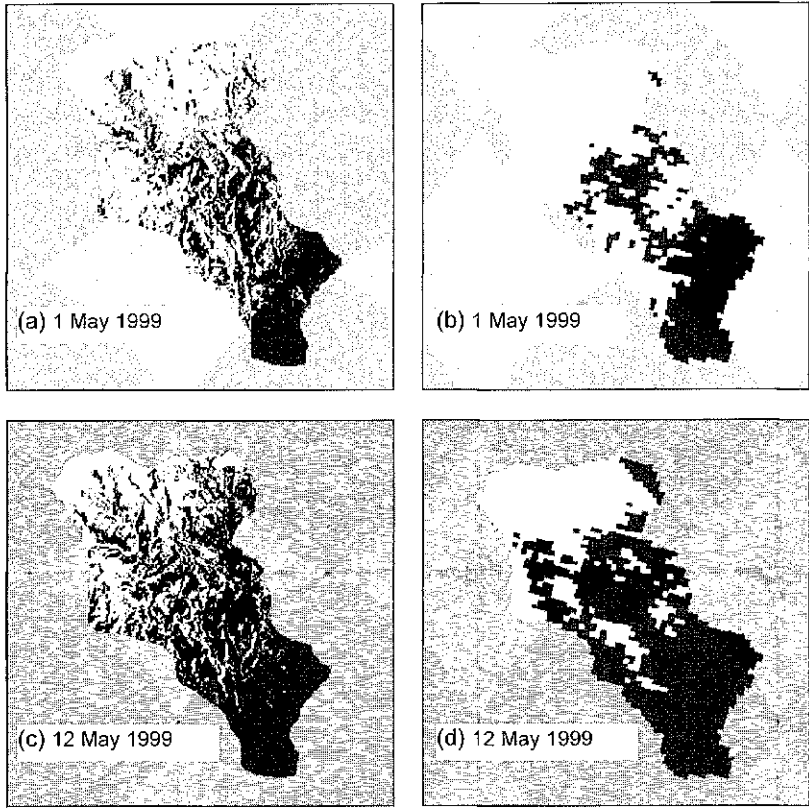


Fig. 5 Comparison of the snow coverage area obtained from orthographic aerial photographs (a) and (c), and the calculated snow coverage area (b) and (d). (a) and (b) are the snow distributions on 1 May 1999, (c) and (d) are those on 12 May 1999.

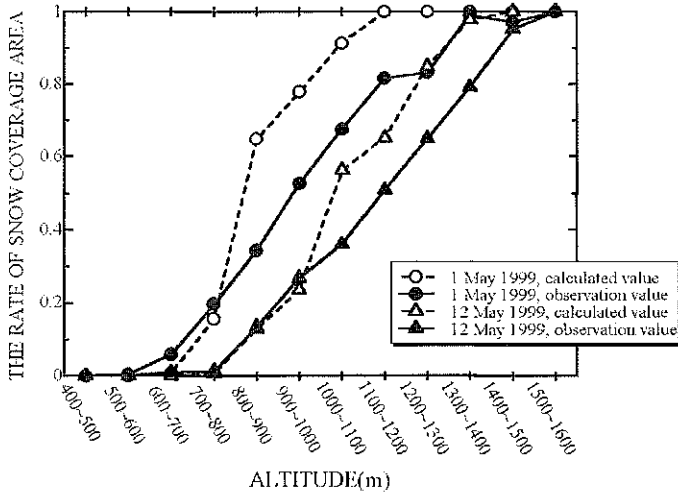


Fig. 6 The rate of snow coverage for each altitude zone.

CONCLUSIONS

The model performed quite well in the low altitude zone and it was able to determine the snow water equivalent at forest sites at high altitude. Conversely, the simulation results were poor for open sites at high altitude. It is thought that the wind causes snow redistribution at high altitudes; this effect was not included in the model. The spatial distribution of snow in the basin was simulated accurately, and the simulated snow line was in good agreement with the actual snow line.

REFERENCES

- Kojima, K. (1957) Viscous compression of a natural snow layer III. *Low Temp. Sci. series A* **16**, 106–109 (in Japanese).
- Kondo, J. & Yamazaki, T. (1990) A prediction model for snow melt, snow surface temperature and freezing depth using a heat balance method. *J. Appl. Met.* **29**, 375–384.
- Ohta, T. (1989) Estimation of the water equivalent of snow cover in a mountainous region from precipitation and daily mean temperature. *Seppyo* **51**, 37–48 (in Japanese with an English summary).
- Ohta, T. (1992) Prediction of net radiation on the snow surface and surface snowmelt rates at an open site and a forest site. *J. Japan Soc. Hydrol. & Water Resour.* **5**(4), 19–26 (in Japanese with an English summary).
- Ohta, T. (1994) A distributed snowmelt prediction model in mountain areas based on an energy balance method. *Ann. Glaciol.* **19**, 107–113.
- Ohta, T., Hashimoto, T. & Ishibashi, H. (1993) Energy budget comparison of snowmelt rates in a deciduous forest and an open site. *Ann. Glaciol.* **18**, 53–59.
- Suzuki, K., Ohta, T., Kojima, A. & Hashimoto, T. (1999) Variation in snowmelt energy and balance characteristics with larch forest density on Mt Iwate, Japan: observation and energy balance analyses. *Hydrol. Processes* **13**, 2675–2688.